



## Review

**Modeling the early signaling events mediated by FcεRI**

Byron Goldstein<sup>a,\*</sup>, James R. Faeder<sup>a</sup>, William S. Hlavacek<sup>a</sup>,  
Michael L. Blinov<sup>a,b</sup>, Antonio Redondo<sup>c</sup>, Carla Wofsy<sup>a,d</sup>

<sup>a</sup> *Theoretical Biology and Biophysics Group, Theoretical Division, Los Alamos National Laboratory, Los Alamos, NM 87545, USA*

<sup>b</sup> *Faculty of Mathematics and Computer Science, Weizmann Institute of Science, Rehovot 76100, Israel*

<sup>c</sup> *Theoretical Chemistry and Molecular Physics Group, Theoretical Division, Los Alamos National Laboratory, Los Alamos, NM 87545, USA*

<sup>d</sup> *Department of Mathematics and Statistics, University of New Mexico, Albuquerque, NM 87131, USA*

Received 28 December 2001; accepted 21 January 2002

**Abstract**

We present a detailed mathematical model of the phosphorylation and dephosphorylation events that occur upon ligand-induced receptor aggregation, for a transfectant expressing FcεRI, Lyn, Syk and endogenous phosphatases that dephosphorylate exposed phosphotyrosines on FcεRI and Syk. Through model simulations we show how changing the ligand concentration, and consequently the concentration of receptor aggregates, can change the nature of a cellular response as well as its amplitude. We illustrate the value of the model in analyzing experimental data by using it to show that the intrinsic rate of dephosphorylation of the FcεRI γ immunoreceptor tyrosine-based activation motif (ITAM) in rat basophilic leukemia (RBL) cells is much faster than the observed rate, provided that all of the cytosolic Syk is available to receptors.

Published by Elsevier Science Ltd.

*Keywords:* Receptor aggregation; Signal transduction; Mathematical modeling; FcεRI; Lyn; Syk

**1. Introduction**

We present a detailed mathematical model of the early signaling events triggered by the aggregation of the high affinity receptor for IgE, FcεRI. We view mathematical models of signaling cascades, such as the one we present, as analogous to stable transfectants. In both the model and the transfectant, a small subset of the molecules that participate in the signal cascade are selected for study. The role of both the model and the transfectant is to understand how the selected molecules interact with each other. However, unlike creating a transfectant, building a model requires explicitly defining all the interactions that can occur and the rates at which they proceed. To use the model to make predictions, the equivalent of doing experiments with a transfectant, one must assign values for the rate constants that characterize the interactions and for the concentrations of the interacting molecules at the start of the experiment. It is then through comparison of model predictions with the experimental data that the interactions and rate constants of the model are tested and, if need be, revised.

The mathematical model we describe in the next sections is a beginning. We anticipate that it will grow in complexity as we add additional participating molecules and interactions in an attempt to encompass more and more of the known signaling cascade. Here we illustrate how we are using the model to make quantitative predictions for experiments in progress in Henry Metzger's laboratory on Chinese hamster ovary (CHO) cells transfected with FcεRI, Lyn and Syk.

**2. Components of the model**

The composition of a mathematical model is determined by the experimental system of interest and the kinds of experiments one wishes to use the model to analyze. Our experimental system is a CHO cell transfected with FcεRI, Lyn and Syk. Our model components are these three molecules plus the simplest ligand that can induce receptor aggregation, a symmetric bivalent ligand. In addition, there is a pool of phosphatases present that dephosphorylate accessible phosphotyrosines. The model considers an ideal transfectant, one that has no endogenous proteins other than the phosphatases that interact with the proteins being studied.

Much of the data that we will analyze will involve the phosphorylation and dephosphorylation of the FcεRI β and

\* Corresponding author. Tel.: +1-505-667-6538; fax: +1-505-665-3493.  
E-mail address: bxg@lanl.gov (B. Goldstein).

$\gamma$  immunoreceptor tyrosine-based activation motifs (ITAMs) and of the tyrosines on Syk. Although an ITAM has two canonical tyrosines and the  $\beta$  ITAM of Fc $\epsilon$ RI has a third tyrosine, we treat an ITAM as a single unit that is either phosphorylated or not. We go further and lump the two ITAMs on the disulfide-bonded  $\gamma$  chains into a single unit. Nothing is known about the stoichiometry of Syk binding to phosphorylated  $\gamma_2$ . Since Syk has a mass that is eight times that of the cytoplasmic domains of the  $\gamma$  chain dimer, we assume that only one Syk can bind to a receptor.

Lyn has two tyrosines but the model does not include the reactions by which they become phosphorylated and dephosphorylated. Thus, in its present form, the model cannot be used to analyze data concerning the phosphorylation of Lyn. Syk has at least 10 tyrosines that become phosphorylated upon receptor aggregation (Furlong et al., 1997). We lump these tyrosines into two groups, those that are primarily phosphorylated by Lyn and those that are primarily phosphorylated by Syk.

At present the model considers only cases where the receptor is monovalent and the ligand is symmetric and bivalent, such as when the ligand is a dimer of IgE or when the  $\alpha$  chain is complexed with a bispecific IgE and the ligand is bivalent and symmetric, and therefore, binds to only one of the Fab sites on the IgE. In the latter case, the  $\alpha$  subunit in the model is the  $\alpha$  chain complexed with the bispecific IgE.

### 3. Reactions of the model

Metzger et al. (2001), in this volume, have reviewed the experimental results that form the basis of our model. Fig. 1 shows the binding and dissociation reactions and Fig. 2 the phosphorylation and dephosphorylation reactions that we include in the model. All the reactions occur at the plasma membrane, except the dephosphorylation of phosphorylated Syk that has dissociated from the receptor. The reverse arrows in Fig. 2 indicate dephosphorylation reactions. The phosphatases responsible for these reactions are not identified in the model but their effects are included as rates of dephosphorylation that are constant in time. We are, therefore, assuming that the interacting phosphatases are in excess so that their concentrations remain constant over the times of the experiments we study.

The binding reactions involving Lyn and Syk with Fc $\epsilon$ RI, i.e. constitutive association of Lyn through its unique domain with the unphosphorylated  $\beta$  chain, recruitment of Lyn to the phosphorylated  $\beta$  ITAM, and recruitment of Syk to the phosphorylated  $\gamma$  ITAM, are well documented (Jouvin et al., 1994; Kihara and Siraganian, 1994; Yamashita et al., 1994; Shiue et al., 1995a; Lin et al., 1996; Vonakis et al., 1997, 2001; Ottinger et al., 1998). Since the  $\alpha\gamma_2$  form of Fc $\epsilon$ RI is phosphorylated by Lyn (Lin et al., 1996), Lyn may also associate constitutively with the unphosphorylated  $\gamma$  chain. This association, if it occurs, is much weaker than the Lyn- $\beta$

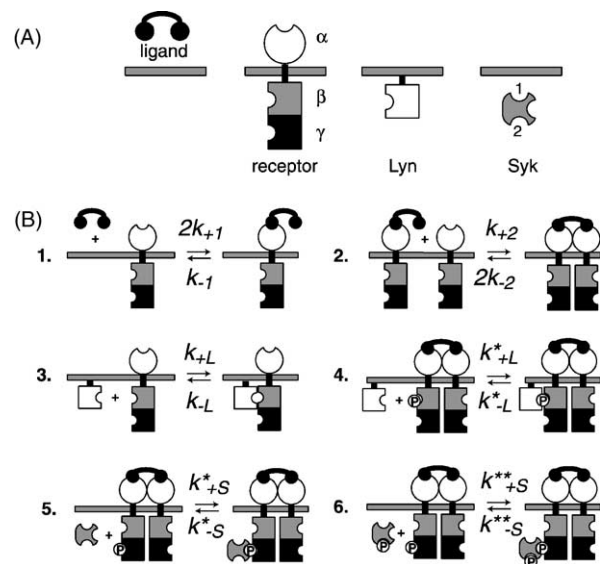


Fig. 1. The binding reactions. (A) The four components of the model. They are represented in this way for ease in displaying the reactions of the model. Site 1 on Syk represents all tyrosines that are phosphorylated by Lyn and site 2 on Syk represents all tyrosines that are phosphorylated by Syk. (B) Binding reactions and their rate constants. (1) Ligand binding: a site on a bivalent ligand binds reversibly to the receptor with forward and reverse rate constants  $k_{+1}$  and  $k_{-1}$ . (2) Ligand induced receptor aggregation: a free site on a ligand with one site bound to a receptor binds reversibly to a second receptor with rate constants  $k_{+2}$  and  $k_{-2}$ . (3) Constitutive association of Lyn: Lyn binds reversibly to the unphosphorylated  $\beta$  subunit with rate constants  $k_{+L}$  and  $k_{-L}$ . (4) Recruitment of Lyn: Lyn binds reversibly to the phosphorylated  $\beta$  ITAM with rate constants  $k_{+L}^*$  and  $k_{-L}^*$ . (5 and 6) Recruitment of Syk: Syk not phosphorylated by Syk binds reversibly to the phosphorylated  $\gamma$  ITAM with rate constants  $k_{+S}^*$  and  $k_{-S}^*$ . Syk phosphorylated by Syk binds reversibly to the phosphorylated  $\gamma$  ITAM with rate constants  $k_{+S}^{**}$  and  $k_{-S}^{**}$ . An asterisk indicates a binding or dissociation reaction with a phosphorylated ITAM. A double asterisk indicates a binding or dissociation reaction involving autophosphorylated Syk and a phosphorylated  $\gamma$ .

chain interactions (Vonakis et al., 1997) and is expected to play an insignificant role when the receptor is  $\alpha\beta\gamma_2$ .

Upon aggregation of Fc $\epsilon$ RI, tyrosines on the  $\beta$  and  $\gamma$  chains of the receptor become phosphorylated and, when disaggregation is induced, become dephosphorylated (Paolini et al., 1991). The substrates for the phosphorylation and dephosphorylation reactions in the model are the  $\beta$  and  $\gamma$  ITAMs of the receptor and two blocks of sites on Syk, the first containing all tyrosines that can be phosphorylated by Lyn and the second containing all tyrosines that can be phosphorylated by Syk. In the model, all the phosphorylation reactions take place at the receptor and all the reactions are trans, i.e. Lyn and Syk cannot phosphorylate substrates that are associated with any of the chains of the receptors they are associated with. Transphosphorylation of the receptor by Lyn has been demonstrated (Pribluda et al., 1994) but it is less clear whether the autophosphorylation of Syk requires two Syk molecules to be on two different receptors in an aggregate. There is indirect evidence that autophosphorylation of Syk is trans (El-Hillal et al., 1997), however, for the

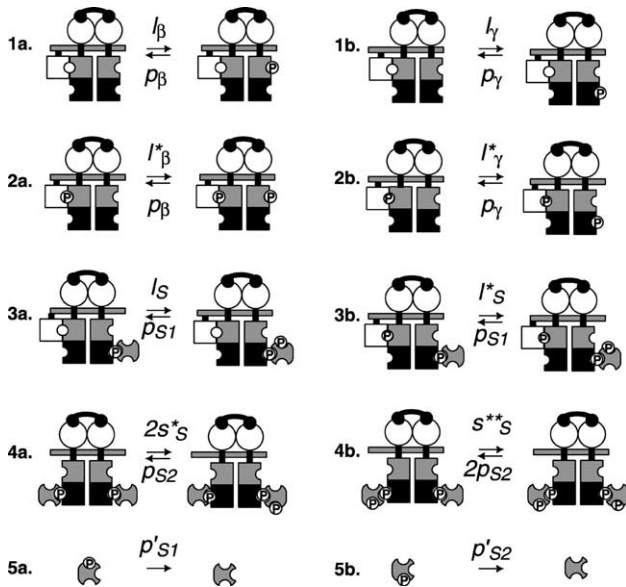


Fig. 2. The Phosphorylation and Dephosphorylation Reactions.  $l$  and  $s$  represent the rate constants for phosphorylation reactions carried out by Lyn and Syk, respectively, and  $p$  the rate constants for dephosphorylation reactions carried out by phosphatases. An asterisk indicates that the kinase is bound to a phosphorylated ITAM. A double asterisk indicates Syk is bound to a phosphorylated ITAM and it has been phosphorylated by Syk making it more active than a Syk that has not been autophosphorylated. (1) Constitutively associated Lyn transphosphorylates (a) the  $\beta$  ITAM with rate constant  $l_{\beta}$  and (b) the  $\gamma$  ITAM with rate constant  $l_{\gamma}$ . (2) Lyn bound to a phosphorylated  $\beta$  ITAM transphosphorylates (a) the  $\beta$  ITAM with rate constant  $l_{\beta}^*$  and (b) the  $\gamma$  ITAM with rate constant  $l_{\gamma}^*$ . The rate constants for dephosphorylation are  $p_{\beta}$  and  $p_{\gamma}$ . (3a) Constitutively associated Lyn transphosphorylates Syk with rate constant  $l_s$  and (3b) Lyn bound to a phosphorylated  $\beta$  ITAM transphosphorylates Syk with rate constant  $l_s^*$ . The rate constant for dephosphorylation is  $p_{S1}$ . (4a) Syk bound to a phosphorylated  $\gamma$  ITAM transphosphorylates Syk with rate constant  $s_s^*$ . (4b) Activated Syk (a Syk phosphorylated by Syk) transphosphorylates Syk with rate constant  $s_s^{**}$ . The rate constant for dephosphorylation is  $p_{S2}$ . (5) Dephosphorylation of Syk in solution a. with rate constant  $p'_{S1}$  for the sites on Syk phosphorylated by Lyn and b. with rate constant  $p'_{S2}$  for the sites on Syk phosphorylated by Syk.

related kinase ZAP-70 it has been suggested that one role of the T cell receptor tandem  $\zeta$  chain ITAMs is to facilitate the autophosphorylation of ZAP-70 (Neumeister et al., 1995). Since there are two  $\gamma$  ITAMs per Fc $\epsilon$ RI a similar possibility exists. In the model we assume, on steric grounds, that this does not occur.

Only Lyn phosphorylates the receptor ITAMs (Nishizumi and Yamamoto, 1997). When the three tyrosines in the  $\beta$  ITAM are changed to phenylalanines, the  $\gamma$  ITAM still becomes phosphorylated (Lin et al., 1996) indicating that constitutively associated Lyn can phosphorylate both the  $\beta$  and  $\gamma$  ITAMs (Fig. 2, reactions (1a) and (1b)). We assume this is also the case when Lyn is bound to the phosphorylated  $\beta$  ITAM (Fig. 2, reactions (2a) and (2b)).

Syk can be phosphorylated by both Lyn and Syk (Keshvara et al., 1998). The roles of the specific tyrosines on Syk are reviewed by Siriganian et al. in this volume. The binding of Syk to the diphosphorylated  $\gamma$  ITAM is

sufficient to activate Syk (Rowley et al., 1995; Shiue et al., 1995b). Further activation of Syk, which is required for rat basophilic leukemia (RBL) cell degranulation, occurs when Syk is phosphorylated by Syk (Fig. 2, reaction (4)) at two adjacent tyrosines in the Syk activation loop (Zhang et al., 2000; Siriganian et al., 2001).

#### 4. Implementing the model

There are two general approaches for taking the components and reactions of Figs. 1 and 2 and converting them into a predictive mathematical model. One applies deterministic methods where processes are described through chemical rate equations (a system of ordinary differential equations) and predictions are made about how average concentrations change in time. For the same set of parameter values, solving these equations always gives the same answer. A second approach applies stochastic methods, where processes are described using probability distributions (Gillespie, 1976). With a stochastic model, for the same set of parameters, each simulation yields a different answer. Doing many simulations with the same set of parameters and averaging the results gives a prediction about how average concentrations change in time and, in addition, how concentrations fluctuate in time. The two methods complement each other, each having advantages and disadvantages. We have used both methods, but the results we present here are generated using the deterministic form of the model.

Fig. 3 shows all the reactions that a particular state of the model, an unphosphorylated receptor dimer with one Lyn bound constitutively, can participate in. Note that the reactions couple it to nine other states and that these states are coupled with a comparable number of states. When a

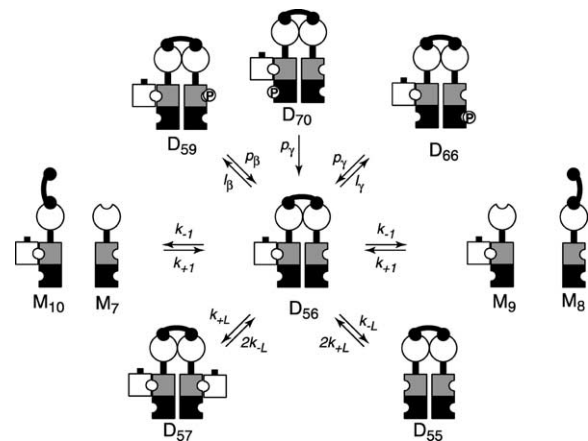


Fig. 3. Reactions involving the dimer state in which both receptors are unphosphorylated and one Lyn is constitutively associated.  $M$  and  $D$  stand for monomer and dimer state concentrations. There are 354 states in the model and each state is assigned a number by the computer algorithm used to generate the rate equations. For example,  $D_{56}$  represents the concentration of the unphosphorylated dimer state with one constitutively associated Lyn. Eq. (1) is written in terms of these concentrations.

ligand induces receptor aggregation, a complex chemical network is set up. This network arises because a scaffolding of signaling molecules, in our case Lyn and Syk, associates with the receptor, leading to a large number of possible states. *In such a signaling cascade there are a multitude of paths that go from receptor aggregation to some final outcome.*

In this model, there are 300 dimer states, 48 monomer states and 6 non-receptor states (free ligand, unassociated Lyn, and cytosolic Syk that is unphosphorylated, phosphorylated only by Lyn, phosphorylated only by Syk, and phosphorylated by Lyn and Syk). The mathematical model consists of 354 chemical rate equations plus initial conditions, i.e. the concentrations of ligand, free receptor and receptor constitutively associated with Lyn, free Lyn, and Syk at the start of the experiment. For example, the equation for the state shown in Fig. 3 is

$$\begin{aligned} \frac{dD_{56}}{dt} = & k_{+1}M_{10}M_7 - k_{-1}D_{56} + k_{+1}M_9M_8 - k_{-1}D_{56} \\ & + 2k_{+L}LD_{55} - k_{-L}D_{56} - k_{+L}LD_{56} + 2k_{-L}D_{57} \\ & - l_{\beta}D_{56} + p_{\beta}D_{59} - l_{\gamma}D_{56} + p_{\gamma}D_{66} + p_{\gamma}D_{70} \end{aligned} \quad (1)$$

We have developed an algorithm that generates the rate equations automatically from the classes of reactions specified in Figs. 1 and 2.<sup>1</sup> For a given set of parameter values and initial conditions these coupled equations are solved numerically.

## 5. Parameter values used in simulations

The parameter values we use in the simulations in the following sections are given in Table 1, which is still “a work in progress.” We anticipate that through comparison of model predictions with experiments done in Henry Metzger’s laboratory, with transfectants expressing FcεRI, Lyn and Syk, an improved set of values will result. In the next section, we illustrate how the model is used to estimate parameter values by showing how we arrived at the values for the rate constants for dephosphorylation of the β and γ ITAMs, the dephosphorylation reactions (2a) and (2b) in Fig. 2.

## 6. Dephosphorylation and protection from dephosphorylation

When the aggregates of IgE on RBL cells are induced to disaggregate, by the addition of high concentrations of monovalent hapten, the receptors dephosphorylate rapidly. Mao and Metzger (1997), using RBL cells, determined the rates of β and γ dephosphorylation to be 0.12 and 0.06 s<sup>-1</sup>. These observed rates of dephosphorylation depend on the relevant phosphatases and on the rates of binding and dissociation of Lyn and Syk, since SH2 domains bound to phos-

Table 1  
Parameter values

Parameter	Value
<b>Components<sup>a</sup></b>	
$N_{\text{receptor}}$ (number of receptors per cell) <sup>b</sup>	$4.0 \times 10^5$
$N_{\text{Lyn}}$ (number of Lyn per cell) <sup>c</sup>	$2.8 \times 10^4$
$N_{\text{Syk}}$ (number of Syk per cell) <sup>b</sup>	$1.6 \times 10^6$
<b>Ligand binding<sup>c</sup></b>	
$k_{+1}$ (M <sup>-1</sup> s <sup>-1</sup> )	$8.0 \times 10^4$
$k_{-1} = k_{-2}$ (s <sup>-1</sup> )	$1.0 \times 10^{-5}$
$k_{+2}$ (s <sup>-1</sup> per molecule)	$2.5 \times 10^{-4}$
<b>Lyn association</b>	
$k_{+L} = k_{+L}^*$ (s <sup>-1</sup> per molecule)	$5.0 \times 10^{-5}$
$k_{-L}$ (s <sup>-1</sup> )	$2.0 \times 10^1$
$k_{-L}^*$ (s <sup>-1</sup> )	$1.0 \times 10^{-1}$
<b>Syk association<sup>d</sup></b>	
$k_{+S}^* = k_{+S}^{**}$ (M <sup>-1</sup> s <sup>-1</sup> )	$1.6 \times 10^7$
$k_{-S}^*$ (s <sup>-1</sup> )	$5.0 \times 10^{-2}$
$k_{-S}^{**}$ (s <sup>-1</sup> )	$1.0 \times 10^{-1}$
<b>Phosphorylation<sup>e</sup></b>	
$l_{\beta} = l_{\gamma} = l_{\beta}^* = l_{\gamma}^* = l_S = l_S^*$ (s <sup>-1</sup> )	$1.0 \times 10^2$
$s_S^*$ (s <sup>-1</sup> )	$1.0 \times 10^2$
$s_S^{**}$ (s <sup>-1</sup> )	$2.0 \times 10^2$
<b>Dephosphorylation</b>	
$p_{\beta} = p_{\gamma} = p_{\beta}^* = p_{\gamma}^* = p_{S1} = p_{S2} = p'_{S1} = p'_{S2}$ (s <sup>-1</sup> )	$1.0 \times 10^2$

<sup>a</sup> Simulations were performed assuming a cell density of  $1 \times 10^6$  cells ml<sup>-1</sup>.

<sup>b</sup> Reischl and Metzger, unpublished observations.

<sup>c</sup> Wofsy et al. (1997).

<sup>d</sup> Rate constants characterizing Syk recruitment were chosen to be consistent with the measured equilibrium constant for Syk-ITAM binding at 25 °C (Ottinger et al., 1998). The cell volume was taken to be  $1.4 \times 10^{-9}$  ml, so the initial Syk concentration equals  $1.9 \times 10^{-6}$  M. The rate constants  $k_{-S}^*$  and  $k_{-S}^{**}$  ( $k_{-S}^{**} > k_{-S}^*$ ) were chosen to be consistent with the observation that autophosphorylated Syk dissociates faster than non-autophosphorylated Syk (Keshvara et al., 1998).

<sup>e</sup> The rate constants  $s_S^*$  and  $s_S^{**}$  ( $s_S^{**} > s_S^*$ ) were chosen to be consistent with the observation that autophosphorylated Syk is more active than non-autophosphorylated Syk when bound to the γ ITAM (Zhang et al., 2000).

phosphotyrosines block dephosphorylation (Rotin et al., 1992). The observed dephosphorylation rates give us lower bounds on the rates of dissociation of Lyn and Syk from their respective phosphorylated ITAMs,  $k_{-L}^*$  and  $k_{-S}^*$ , neither of which has been directly determined. As a starting point we take  $k_{-L}^* = 0.1 \text{ s}^{-1}$  and  $k_{-S}^* = 0.05 \text{ s}^{-1}$  which correspond with mean times of 10 s for Lyn and 20 s for Syk to remain bound to phosphorylated ITAMs. Fig. 4 shows predicted dephosphorylation curves after hapten addition, for different values of the dephosphorylation rate constants. Because there are  $1.6 \times 10^6$  Syk<sup>2</sup> and  $4 \times 10^5$  FcεRI per RBL cell, we expect Syk, by binding to the phosphorylated γ ITAM, to dramatically slow the rate of γ dephosphorylation. We previously estimated that in RBL cells only about  $2.8 \times 10^4$  Lyn molecules are available to interact with re-

<sup>1</sup> Hlavacek et al., unpublished result.

<sup>2</sup> Reischl and Metzger, unpublished observations.

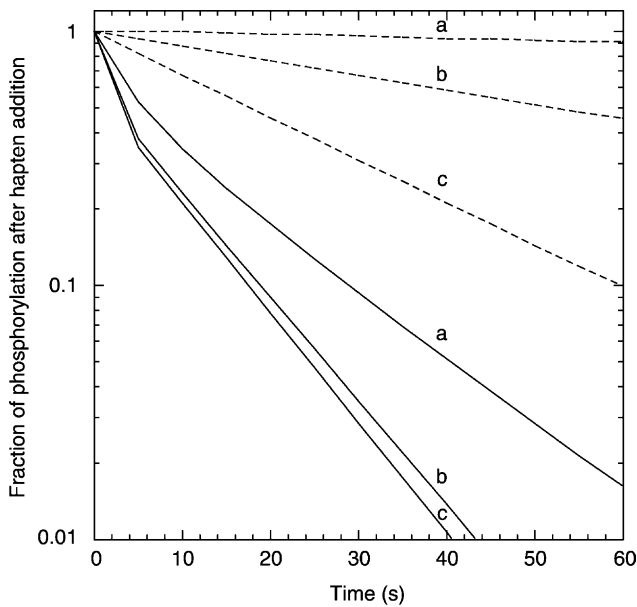


Fig. 4. Simulation of the time course of dephosphorylation of the  $\beta$  and  $\gamma$  ITAMs of Fc $\epsilon$ RI after dimeric aggregates of IgE are disaggregated. A rapidly reversible bivalent ligand ( $k_{+1} = 1.2 \times 10^7 \text{ M}^{-1} \text{ s}^{-1}$ ,  $k_{-1} = 0.5 \text{ s}^{-1}$ ) at a concentration of 10 nM was allowed to bind for 2 min to RBL cells sensitized with a bispecific IgE at which time binding was instantly blocked. Shown are time courses for dephosphorylation of the  $\gamma$  ITAM (dotted line) and  $\beta$  ITAM (solid line) for the dephosphorylation rate constant ( $p_{\beta} = p_{\gamma}$ ) equal to (a)  $1.0 \text{ s}^{-1}$ , (b)  $10 \text{ s}^{-1}$ , and (c)  $100 \text{ s}^{-1}$ . Other parameters used in the simulation are given in Table 1. For  $p_{\beta} = 100 \text{ s}^{-1}$  the slope of the  $\beta$  dephosphorylation curve after the initial transition is  $0.10 \text{ s}^{-1}$ , the value of the rate constant,  $k_{+L}^*$ , for the dissociation of recruited Lyn (Table 1). When disaggregation occurs ( $t = 0$ ) some phosphorylated  $\beta$  ITAMs are exposed and some have Lyn bound. The transients (solid line, a, b and c) arise from dephosphorylation of the unprotected  $\beta$  ITAMs while the remainder of the curve is determined by Lyn dissociation from the phosphorylated  $\beta$  ITAM. For  $p_{\gamma} = 100 \text{ s}^{-1}$  the slope of the  $\gamma$  dephosphorylation curve is  $0.04 \text{ s}^{-1}$ , still somewhat slower than  $0.05 \text{ s}^{-1}$ , the value of the rate constant,  $k_{-S}^*$ , for dissociation of Syk from the phosphorylated  $\gamma$  ITAM (Table 1). Because of the high Syk concentration, even with  $p_{\gamma} = 100 \text{ s}^{-1}$ , there is some rebinding of Syk to phosphorylated  $\gamma$  before dephosphorylation occurs. This effect becomes dramatic when  $p_{\gamma}$  is reduced (dotted line, a and b).

ceptors (Wofsy et al., 1997). Therefore, we expect Lyn to be much less effective at slowing dephosphorylation of  $\beta$ . The model predictions (Fig. 4) bear this out. Dephosphorylation of  $\gamma$  is more sensitive to the value of the dephosphorylation rate constant than is dephosphorylation of  $\beta$ . To see  $\gamma$  dephosphorylation on the time scale observed experimentally, the dephosphorylation rate must be fast enough for dephosphorylation of an exposed phosphorylated ITAM to occur before Syk binds and protects the site from dephosphorylation. Assuming that the dephosphorylation rate constants for the  $\beta$  and  $\gamma$  ITAMs,  $p_{\beta}$  and  $p_{\gamma}$ , are equal, to obtain reasonable agreement with the observed dephosphorylation rates (Mao and Metzger, 1997) we need to take  $p_{\beta} = p_{\gamma} \geq 100 \text{ s}^{-1}$ , or about 1000 times faster than the observed rates. We must choose such a high value for the dephosphorylation rate constant because so much Syk is available to the

receptors. However, if much of the Syk is sequestered, i.e. not available to the aggregated Fc $\epsilon$ RI, then this would also explain the lack of protection afforded the phosphorylated  $\gamma$  ITAM by Syk during dephosphorylation (Mao and Metzger, 1997).

## 7. Changes in ligand concentration can change the nature of a response

One role of a detailed mathematical model is to make quantitative predictions. We illustrate this by considering two hypothetical transfectants that are exposed to IgE dimers for 10 min. One (Fig. 5a and b) has the same number of receptors, available Lyn and Syk, that we believe an RBL cell has. For RBL cells, in terms of numbers per cell: Syk > Fc $\epsilon$ RI > Lyn (available). One testable prediction (Fig. 5a) is that the ratio of phosphorylated  $\gamma$  to  $\beta$  is an increasing function of the concentration of IgE dimers on the cell surface. (In Fig. 5a, the ratio of phosphorylated  $\gamma$  to  $\beta$  increases from 2.4 to 11.5 for the ligand concentrations shown.) Since the model includes the molecules (Lyn, Syk and the pool of phosphatases) known to interact directly with the receptor ITAMS, we expect this prediction to apply to RBL cells.

The model also predicts (Fig. 5b) that changing the ligand concentration changes not only the concentration of phosphorylated Syk but also the relative concentrations of individual phosphotyrosines on Syk. Simulations show that the ratio of those tyrosines on Syk phosphorylated by Syk to those phosphorylated by Lyn changes as the ligand concentration changes. Since different signaling molecules associate with different phosphotyrosines, the model illustrates how different concentrations of the same ligand can trigger different cellular responses. *Changing the concentration of receptors in aggregates can change not only the amplitude of a cellular response but also the nature of the response.* (The quantitative prediction (Fig. 5b) only applies to the hypothetical transfectant, not to an RBL cell, since none of the molecules that associate with Syk, other than the receptor, are in the model.)

In Fig. 5c and d, we consider a transfectant with a much reduced concentration of Syk so that FcRI  $\gg$  Syk = Lyn. In this simulation, the concentration of autophosphorylated Syk goes through a maximum as a function of ligand concentration. This is a consequence of Syk autophosphorylation being trans. The decrease in Syk autophosphorylation when receptor aggregates are in high concentration comes about because under these conditions receptors with phosphorylated  $\gamma$  ITAMS are in excess compared to Syk. In this limit, the probability of having two Syks in the same aggregate passes through a maximum as the number of aggregates is increased. The concentration of Lyn also plays a key role since, if it is too low, a sufficiently high concentration of receptors with phosphorylated  $\gamma$  ITAMS cannot be achieved. Since autophosphorylation of Syk is required for degranulation (Zhang et al., 2000) and degranulation of

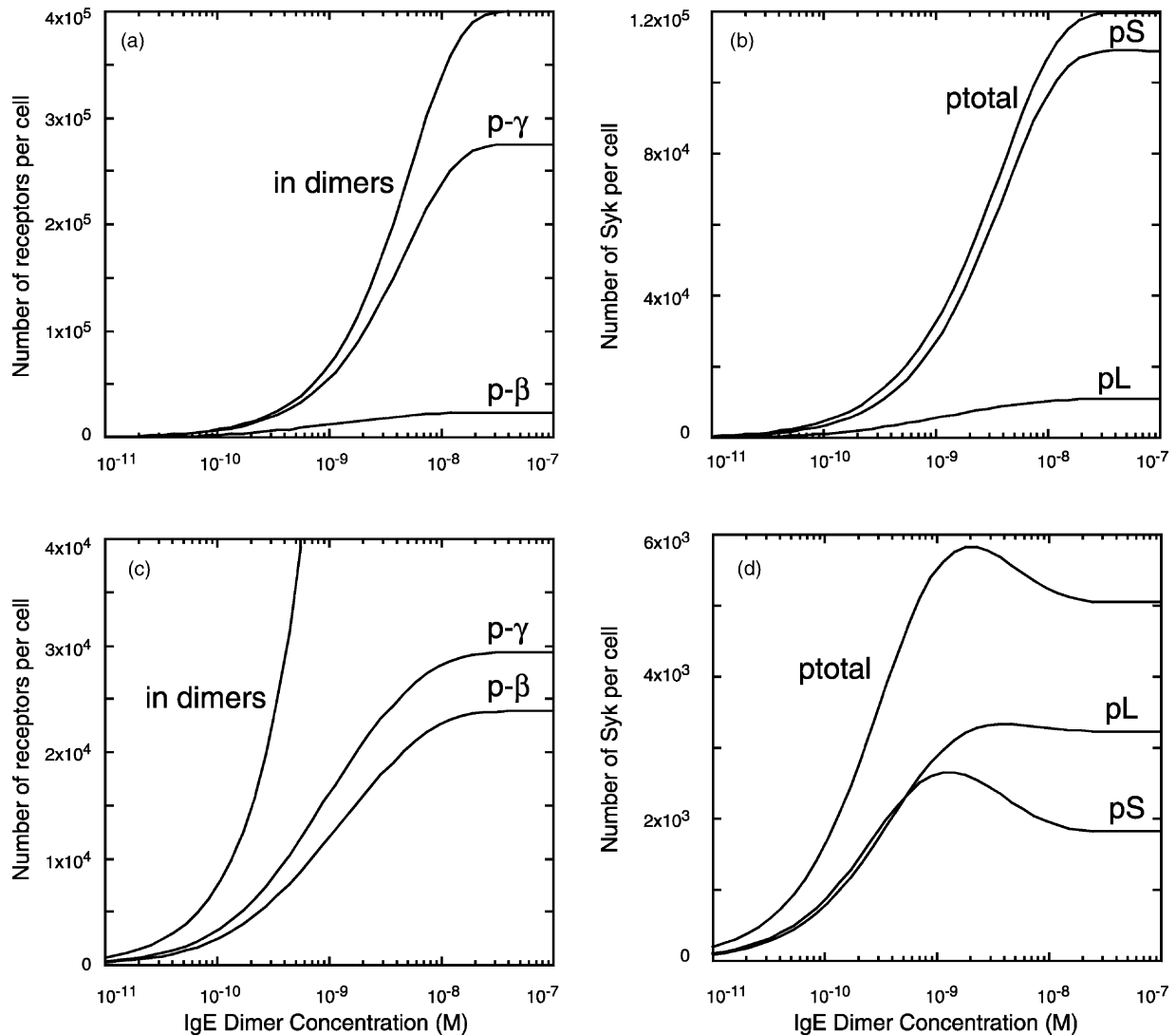


Fig. 5. Simulated dose–response curves for hypothetical transfectants with high (a and b) and low (c and d) Syk concentrations, exposed to IgE dimers for 10 min. In (a) and (b) there are  $1.6 \times 10^6$  Syk per cell and in (c) and (d) there are  $2.8 \times 10^4$  Syk per cell. All other parameters are the same and are given in Table 1. In a and c are plotted the number of IgE in dimers, the number of receptors with their  $\beta$  ITAM phosphorylated (p- $\beta$ ) and the number with their  $\gamma$  ITAM phosphorylated (p- $\gamma$ ). In (b) and (d) the number of Syk molecules phosphorylated by Lyn (pL), by Syk (pS) and the total phosphorylation of Syk (ptotal) are plotted.

basophils can be maximal at submaximal concentrations of receptor aggregation (Magro and Alexander, 1974) as our model suggests Syk can, it would be interesting to know how histamine release dose–response curves compare with dose–response curves for Syk autophosphorylation.

## 8. Conclusions

If we understand a system, then we should be able to predict how it will behave under a variety of experimental conditions. One role of a detailed quantitative model is to assess our understanding, i.e., to keep score of our progress in deciphering how the system works. The building of such a model is a sobering enterprise. It forces us to take stock

of what we do not know about the system and to ask questions that we might never ask if we were not required to describe precisely how we believe the system works. Building the model is a valuable enterprise for this same reason. We anticipate that through collaboration between theory and experiment, mathematical models will become one of the essential tools in the study of cell signaling.

## Acknowledgements

This work was supported by National Institutes of Health grant GM35556 and the US Department of Energy under contract W-7405-ENG-36 through the Los Alamos National Laboratory LDRD program.

## References

- El-Hillal, O., Kurosaki, T., Yamamura, H., Kinet, J.-P., Scharenberg, A.M., 1997. Syk kinase activation by src kinase-initiated activation loop phosphorylation chain reaction. *Proc. Natl. Acad. Sci. USA* 94, 1919–1924.
- Furlong, M.T., Mahrenholz, A.M., Kim, K.-H., Ashendel, C.L., Harrison, M.L., Geahlen, R.L., 1997. Identification of the major sites of autophosphorylation of the murine protein-tyrosine kinase Syk. *Biochim. Biophys. Acta* 1355, 177–190.
- Gillespie, D.T., 1976. A general method for numerically simulating the stochastic time evolution of coupled chemical reactions. *J. Comp. Phys.* 22, 403–434.
- Jouvin, M.-H., Adamczewski, M., Numerof, R., Letourneur, O., Valle, A., Kinet, J.-P., 1994. Differential control of the tyrosine kinases Lyn and Syk by the two signaling chains of the high affinity immunoglobulin E receptor. *J. Biol. Chem.* 269, 5918–5925.
- Keshvara, L.M., Isaacson, C.C., Yankee, T.M., Sarac, R., Harrison, M.L., Geahlen, R.L., 1998. Syk- and Lyn-dependent phosphorylation of Syk on multiple tyrosines following B cell activation includes a site that negatively regulates signaling. *J. Immunol.* 161, 5276–5283.
- Kihara, H., Siraganian, R.P., 1994. Src homology 2 domains of Syk and Lyn bind to tyrosine-phosphorylated subunits of the high affinity IgE receptor. *J. Biol. Chem.* 269, 22427–22432.
- Lin, S., Cicala, C., Scharenberg, A.M., Kinet, J.P., 1996. The FcεRIβ subunit functions as an amplifier of FcεRIγ-mediated cell activation signals. *Cell* 85, 985–995.
- Magro, A.M., Alexander, A., 1974. Histamine release: in vitro studies of the inhibitor region of the dose–response curve. *J. Immunol.* 112, 1762–1765.
- Mao, S.-Y., Metzger, H., 1997. Characterization of protein-tyrosine phosphatases that dephosphorylate the high affinity IgE receptor. *J. Biol. Chem.* 272, 14067–14073.
- Metzger, H., Eglite, S., Haleem-Smith, H., Reischl, I., Torigoe, C., 2001. Quantitative aspects of signal transduction by the receptor with high affinity for IgE. *Mol. Immunol.* 38, 1207–1211.
- Neumeister, E.N., Zhu, Y., Richard, S., Terhorst, C., Chan, A.C., Shaw, A.S., 1995. Binding of Zap-70 to phosphorylated T-Cell receptor ζ and η enhances its autophosphorylation and generates specific binding sites for SH2 domain-containing proteins. *Mol. Cell Biol.* 15, 3171–3178.
- Nishizumi, H., Yamamoto, T., 1997. Impaired tyrosine phosphorylation and Ca<sup>2+</sup> mobilization, but not degranulation, in Lyn-deficient bone marrow-derived mast cells. *J. Immunol.* 158, 2350–2355.
- Ottinger, E.A., Bitfield, M.C., Shoelson, S.E., 1998. Tandem SH2 domains confer high specificity in tyrosine kinase signaling. *J. Biol. Chem.* 273, 729–735.
- Paolini, R., Jouvin, M.-H., Kinet, J.-P., 1991. Phosphorylation and dephosphorylation of the high-affinity receptor for immunoglobulin E immediately after receptor engagement and disengagement. *Nature* 353, 855–858.
- Pribluda, V.S., Pribluda, C., Metzger, H., 1994. Transphosphorylation as the mechanism by which the high-affinity receptor for IgE is phosphorylated upon aggregation. *Proc. Natl. Acad. Sci. USA* 91, 11246–11250.
- Rotin, D., Margolis, B., Daly, R.J., Daum, G., Li, N., Fischer, E.H., Burgess, W.H., Ullrich, A., Schlessinger, H., 1992. SH2 domains prevent tyrosine dephosphorylation of the EGF receptor: identification of tyr 992 as the high-affinity binding site for SH2 domains of phospholipase Cγ. *EMBO J.* 11, 559–567.
- Rowley, R.B., Burhardt, A.L., Chao, H.-G., Matsueda, G.R., Bolen, J.B., 1995. Syk protein-tyrosine kinase is regulated by tyrosine-phosphorylated Igα/Igβ immunoreceptor tyrosine activation motif binding and autophosphorylation. *J. Biol. Chem.* 270, 11590–11594.
- Shiue, L., Green, J., Green, O.M., Karas, J.L., Morgenstern, J.P., Ram, M.K., Taylor, M.K., Soller, M.J., Zydowsky, L.D., Bolen, J.B., Brugge, J.S., 1995a. Interaction of p72<sup>Syk</sup> with the γ and β subunits of the high-affinity receptor for immunoglobulin E, FcεRI. *Mol. Cell Biol.* 15, 272–281.
- Shiue, L., Zoller, M.J., Brugge, J.S., 1995b. Syk is activated by phosphotyrosine-containing peptides representing the tyrosine-based activation motifs of the high affinity receptor for IgE. *J. Biol. Chem.* 270, 10498–10502.
- Siraganian, R.P., Zhang, J., Suzuki, K., Sada, K., 2001. Protein tyrosine kinase Syk in mast cell signaling. *Mol. Immunol.* 38, 1229–1233.
- Vonakis, B.M., Chen, H., Haleem-Smith, H., Metzger, H., 1997. The unique domain as the site on Lyn kinase for its constitutive association with the high affinity receptor for IgE. *J. Biol. Chem.* 272, 24072–24080.
- Vonakis, B.M., Haleem-Smith, H., Benjamin, P., Metzger, H., 2001. Interaction between the unphosphorylated receptor with high affinity for IgE and Lyn kinase. *J. Biol. Chem.* 276, 1041–1050.
- Wofsy, C., Torigoe, C., Kent, Y.M., Metzger, H., Goldstein, B., 1997. Exploiting the difference between intrinsic and extrinsic kinases: implications for regulation of signaling by immunoreceptors. *J. Immunol.* 159, 5984–5992.
- Yamashita, T., Mao, S.-Y., Metzger, H., 1994. Aggregation of the high-affinity IgE receptor and enhanced activity of p53/56<sup>lyn</sup> protein-tyrosine kinase. *Proc. Natl. Acad. Sci. U.S.A.* 91, 11251–11255.
- Zhang, J., Billingsley, M.L., Kincaid, R.L., Siraganian, R.P., 2000. Phosphorylation of Syk activation loop tyrosines is essential for Syk function—an in vivo study using a specific anti-Syk activation loop phosphotyrosine antibody. *J. Biol. Chem.* 275, 35442–35447.